The spectrum of cosmic ray neutrons at sea level in the range 0.4-1.2 GeV

1971 J. Phys. A: Gen. Phys. 4 352

(http://iopscience.iop.org/0022-3689/4/3/013)

J. Phys. A: Gen. Phys., 1971, Vol. 4. Printed in Great Britain

The spectrum of cosmic ray neutrons at sea level in the range 0·4–1·2 GeV

F. ASHTON, H. J. EDWARDS and G. N. KELLY
Department of Physics, University of Durham, Durham, England
MS. received 1*st July* 1970, *in final form* 30*th December* 1970

Abstract. The neutron spectrum at sea level has been measured in the kinetic energy range 0·4–1·2 GeV using the charge exchange reaction $n+p \rightarrow p+n$. In this energy range the vertical intensity of neutrons is found to be consistent with the value calculated from the work of Hughes and Marsden (1966) who estimated the global spectrum of neutrons from indirect measurements of the multiplicity distribution of neutrons in a neutron monitor.

1. Introduction

Apart from its interest as a property of the cosmic radiation, the energy spectrum of neutrons at sea level is important in understanding the propagation of nucleons through the earth's atmosphere. At low energies (< 500 MeV) the energy spectrum has been determined by Hess *et al.* (1959), while in the intermediate energy range (300 MeV to a few GeV) Hughes and Marsden (1966) have estimated the spectrum from indirect measurements of the multiplicity distribution of neutrons in a neutron monitor. At higher energies (> 20 GeV) the spectrum has been obtained from the burst spectrum produced by neutral primary particles in a thick steel target (Ashton and Coats 1968). As the determination in the intermediate energy range is so indirect, the charge exchange reaction $n+p \rightarrow p+n$ has been used to check the conclusions of Hughes and Marsden.

2. The neutron telescope and the basic data

2.1. *The neutron telescope*

A scale diagram of the telescope which is situated under a thin roof 200 feet above sea level is shown in figure 1. It is essentially that used in a search for quarks in the cosmic radiation by Ashton *et al.* (1969) with slight modifications to enable the selection of incident neutral particles.

A–F are plastic scintillators (NE 102A) of dimensions $140 \times 75 \times 5$ cm^3 and are each viewed by six two-inch photomultipliers, three at each 75 cm end, through rectangular (30×75 cm^2) light guides. V is also a plastic scintillator of dimensions $75 \times 30 \times 5$ cm^3 and is viewed through triangular light guides by two two-inch photomultipliers, one at each end. The Čerenkov counters, CII and CI, comprise Perspex boxes of wall thickness $\frac{3}{8}$ inch and external dimensions $149{\cdot}5 \times 86{\cdot}5 \times 18{\cdot}5$ cm^3 filled to a depth of 16·5 cm with distilled water which contained 8 mg/litre of amino G acid to act as a wavelength shifter and hence substantially improve the response of the counter. The Čerenkov light is viewed by eight five-inch photomultipliers, four at each end, placed in optical contact with the 86·5 cm edges of the box. Each tray of neon flash tubes, F_1–F_7, F_a–F_e, contains four layers (apart from F_5 which contains only two) of closely packed tubes of external diameter 1·75 cm and wall thickness 1 mm which are filled to a pressure of 60 cm Hg with commercial grade neon.

2.2. *Selection of events*

It can readily be seen that electronic logic of the type VCDEF $\overline{B}\,\overline{CI}$ would lead to the selection of events in which a neutral particle traverses the region A to CI of the telescope and then a charged particle from V to F. Such a coincidence arrangement

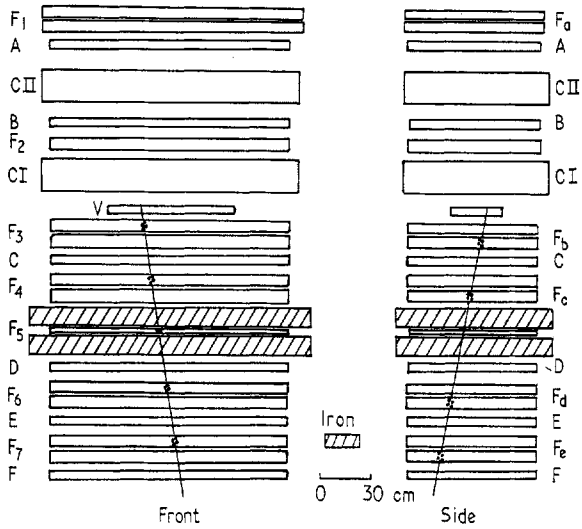

Figure 1. Scale diagram of the telescope used in the N series of measurements. The telescope used in the M series was identical apart from the removal of the iron and F_5. A–F, V are plastic scintillators (NE 102A); CII, CI are water Čerenkov counters; F_1–F_7, F_a–F_e are neon flash tube trays.

was used in the experiment with the following discrimination levels on the counters: 0·25 ν on scintillators C to F, 0·2 ν on scintillator V, 0·05 ν on scintillator B, and 0·5 ν on counter CI, where ν is the most probable pulse height produced in that counter by a relativistic unit-charged particle. This value was found by selecting cosmic ray muons to traverse the telescope with an ABVCDEF coincidence and measuring the pulse height distributions. Using a coincidence VCDEF $\overline{B}\,\overline{CI}$ the target in which the neutral particle can interact is formed by the material between a fraction of counter CI and a fraction of counter V (the fractions depending on the respective discrimination levels on each counter). The composition of the materials comprising the target will be discussed later.

On an event satisfying the electronic logic the pulse from each scintillator and Čerenkov counter is sequentially displayed on an oscilloscope and recorded photographically, and at the same time the flashed tubes in both the side and the front elevations of the telescope are also recorded on film. The recording of the pulse from every counter, not just those involved in the electronic selection, enables counters A and CII to act as independent witnesses of the event, and this lends further support to an interpretation in terms of an incident neutral particle. Further support, also unbiased by the selection system, can be obtained from the twelve layers of flash tubes in trays F_1, F_2 and F_a.

At the completion of the measurements made with the telescope as in figure 1 (to be referred to as the N series of measurements) modifications were made to allow an investigation of lower-energy neutrons. This was accomplished by removing the

steel absorber and flash tube tray F_5 so as to create a lower-energy particle threshold which could traverse the remainder of the telescope after the target region. Otherwise the telescope and electronic logic were identical with those which pertained in the N series. This latter series of measurements is to be referred to as the M series. A summary of the important parameters of the telescope in each series of measurements is given in table 1.

Table 1. Summary of the parameters of the telescope in each series of measurements

(i) *Composition of the target* (N and M series)
8 g cm^{-2} water
1·2 g cm^{-2} Perspex
1·0 g cm^{-2} wood
8·4 g cm^{-2} iron
0·44 g cm^{-2} aluminium
4·13 g cm^{-2} phosphor (NE 102A).

(ii)

	N series	M series
Aperture (cm^2 sr) assuming radiation to have angular variation of $\cos^e\theta$	640	640
Equivalent number of g cm^{-2} H_2O particle has to traverse to penetrate the telescope from the centre of target	194	64·8
Minimum proton kinetic energy required to just traverse the telescope (in MeV)	701	344
Minimum pion kinetic energy required to just traverse the telescope (in MeV)	449	185

In evaluating the minimum energies it is assumed that production occurs at the centre of the target.

2.3. *The basic data and their reduction*

Events were extracted from the photographic records subject to the following criteria:

(i) a track (or burst) should be observed in flash tube-trays F_3–F_7, F_b–F_e, such that it traverses all the scintillators V, C, D, E and F;

(ii) the upward projection of the track (or axis of the burst) must intersect scintillator B;

(iii) there must be no flashed tubes in trays F_1, F_2, or F_a on the upward projection of the track (or axis of the burst);

(iv) there should be no pulse recorded in any of the counters A, CII or B.

Such criteria establish that an observed secondary particle (or particles) has emanated from the interaction of a neutral particle, in all probability a neutron. For each event satisfying the previous conditions the following information was noted: the number of charged particles emerging from the target region; the emission angles of the particle (or axis of the burst) in both elevations; whether or not the particle (or particles) interacts or is scattered in penetrating the telescope; the pulse height recorded by each counter. The basic data referring to the two series of measurements are given in table 2.

Table 2. Basic data referring to the two series of measurements. n is the number of charged prongs leaving the interaction region

	N series	M series
Running time (hours)	140·8	6·03
Mean pressure (mbar)	1003	997
VCDEF rate/hour	$2{\cdot}00 \times 10^4$	$2{\cdot}33 \times 10^4$
B + CI veto rate/hour	$1{\cdot}25 \times 10^7$	$1{\cdot}25 \times 10^7$
Total number of triggers	1865	547
Number of events satisfying the acceptance criteria	363	290
Number with $n = 1$	93	86
Number with $n = 2$	70	72
Number with $n > 2$	200	132

The difference between the total number of triggers and the number of events satisfying the acceptance criteria is accounted for by angled tracks (or showers) traversing scintillators C–F, missing counters A–V, and being accompanied by a random pulse in V, and by weak electron–photon showers.

With regard to establishing incident neutron intensities from the data the only type of event that is particularly useful is that in which $n = 1$. The reason for this stems from the complexity of trying to predict the yield of events with $n > 1$—this arising from the large number of competing channels, as well as their rapidly varying cross sections, in the range of neutron energies currently experienced. The situation is further confused by the marked sensitivity to the energy transferred in the interaction as well as to its distribution among the emerging secondary particles, owing to the rapidly falling neutron spectrum resulting in the majority of energy transfers being close to the minimum required for the particles to traverse the telescope. Thus our attention is confined to those events in which only one charged particle was observed to leave the target region, these events being readily accessible to analysis in that the available production channels are severely restricted and their cross-section variations well known.

The single prong events can be divided up into the following categories:

(i) 'Interacting events'—those in which the secondary particle interacts and more than one charged particle emerges from the interaction region.

(ii) 'Scattered events'—those in which the secondary particle is scattered through more than 4° (this being the minimum angle that could be reliably detected over all regions of the telescope) in either elevation of the telescope and no further charged particle production occurs in the scattering.

(iii) 'Unscattered events'—those which traverse the telescope without deviation ($< 4°$) or interaction.

The breakdown of the single-prong events into these categories is given in table 3 for each series.

A further subdivision of the events in the 'scattered and unscattered' categories can be achieved with resort to the pulse heights measured in the scintillators. Two distinct types of events appear: the first contains particles in which the level of ionization in each counter is significantly greater than the minimum, the level increasing as the particle traverses the telescope; the second contains events where the level remains effectively at minimum throughout the telescope. The particles in the former group have been found to be consistent with being protons from a determination

Table 3. Breakdown of the single-prong events for the two series of measurements

	N series	M series
Total number of single-prong events	93	86
Number 'unscattered'	17	30
Number 'scattered'	47	22
Number 'interacting'	29	34

of their masses using a range–velocity method; the velocity was determined from the measured energy loss and its known variation with velocity, and the mass from the variation of velocity over known amounts of material between each scintillator. This method and its precision in determining masses in the present instrument are described by Kelly (1969).

The condition adopted to separate the two groups ensuring that the former contained a relatively pure sample of protons was that the energy loss in both scintillators E and F should be greater than 1·7 times the minimum. The cleanness of the separation can be seen by considering that a pion ionizing at 1·7 minimum has a residual range of 11 g cm^{-2} water equivalent, whereas the material between E and F is equivalent to 14·7 g cm^{-2} water. Thus a pion satisfying the ionization condition in counter E would be unable to penetrate to F and hence would not be selected. The particles in the latter group are a mixture of pions and protons having sufficient energy to make a separation of them by ionization methods unreliable. Using this method of separation the protons in the first group are constrained to have been produced within well defined energy limits, these being the minimum that is required for the proton to penetrate the whole telescope and such that the energy loss at E is greater than 1·7 times the minimum. The break up of the events into the two groups is given in table 4 with the corresponding energy limits.

Table 4. Breakdown of noninteracting single-prong events showing the number of identified protons

	N series		M series	
	Number	Energy limits	Number	Energy limits
Number of identified protons	25	$701 < E_p < 867$ MeV	28	$344 < E_p < 551$ MeV
Number of protons or pions	39	$E_p > 867$ MeV $E_\pi > 449$ MeV	24	$E_p > 551$ MeV $E_\pi > 185$ MeV

From the raw data containing only the single-prong events, relaxation methods are used to derive neutron intensities; that is, a neutron spectrum and production cross sections are assumed and the expected rates of events are compared with the observations. The major difficulty is in the correction of the predicted rates for losses due to interactions of the secondary particles in penetrating the remainder of the telescope. The calculation procedure and the manner in which corrections were applied for interactions are discussed in the following sections.

3. The expected rates of single-prong events

3.1. *The contributing channels and their cross sections*

In restricting the analysis to single-prong events the number of contributing

channels is limited to two which are the following:

charge exchange $n+p \rightarrow p+n$

and

single pion production $n+p \rightarrow n+n+\pi^+$

with the emergence of neutral nucleons only. All other channels are forbidden—for example multiple pion production, single negative pion production from neutron–neutron interactions—owing to the emergence from the interaction of more than one charged particle.

The only likely contamination of the single-prong sample from channels other than those above arises from the lack of continual visual sensitivity in the target region. It is obviously possible for many charged particles to be produced in the interaction with them all but one being absorbed before emerging into a visually sensitive region of the telescope. Assuming all production to occur at the centre of the telescope, the maximum kinetic energy that a pion or proton can have and not emerge into a visually sensitive part of the telescope is 60 MeV and 130 MeV respectively. From a consideration of the kinematics of the possible channels it is found that the contribution from such effects is not significant.

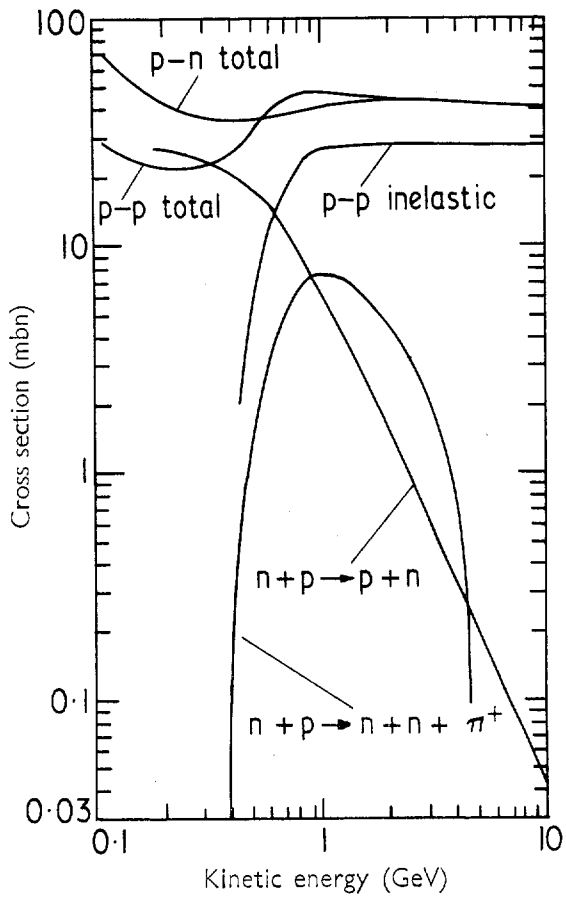

Figure 2. The elementary cross sections used in evaluating the expected yield of single protons and pions. The n–n total cross section is expected to be the same as the p–p total cross section (Galbraith 1969).

The cross sections for the two contributing channels are well known and the variation with neutron energy of those adopted is shown in figure 2. The charge exchange cross section is calculated from the summary of differential cross sections by Manning *et al.* (1966). The cross section for the single pion channel $n+p \rightarrow n+n+\pi^+$ has been derived by multiplying the total np inelastic cross section by the probability of single meson production given by Lindenbaum (1957) and also by the probability of single meson production being the reaction $n+p \rightarrow n+n+\pi^+$ according to its isotopic spin weight. The uncertainties in these adopted values are considered later.

3.2. *The trial neutron spectrum*

As discussed in the introduction there exist at present no direct measurements of the sea level neutron spectrum in the energy region currently of interest. The best estimate presently available comes from the work of Hughes and Marsden (1966) who have radically modified the results of Hess *et al.* (1959).

Hess *et al.* have given the spectrum from thermal energies to 10 GeV, but in fact their spectrum is based on measurements made only up to about 500 MeV. In the range 10 keV to 1 MeV they used trial and error procedures to find the shape of the spectrum that would uniquely reproduce the observations. Beyond 1 MeV similar methods were used but as a guide to the shape they assumed the exponent of the spectrum at energies above 3 GeV to be 2·15, the same as the exponent of the primary spectrum given by Singer (1958). However, later measurements of the sea level proton spectrum by Brooke and Wolfendale (1964) have shown the exponent to be approximately 2·6 in the energy range 10–100 GeV, and it is expected that the neutron and proton spectra will become identical in such an energy range. It is thus apparent that Hess *et al.* had seriously overestimated the spectrum at higher energies, and Hughes and Marsden compensated for this by adopting the Hess spectrum up to 200 MeV and then adjusting the slope until it approached a value of 2·6 at around 10 GeV. A reiterative procedure was used to optimize the shape of the spectrum in this intermediate region by obtaining the best fit between the multiplicity spectrum observed with their neutron monitor and that predicted from the chosen spectral shape. An evaluation of the spectrum in this manner however is particularly sensitive to the interaction probability, the monitor efficiency and the neutron multiplicity as a function of incident energy that are adopted, and the final spectrum must therefore remain somewhat uncertain. Account of neutron production by protons, muons, pions etc., has also to be accounted for with this procedure. In fact it would appear that they have underestimated the neutron spectrum in that they have used a geometrical cross section rather than the inelastic cross section (elastic interactions, by definition, not contributing) in evaluating interaction probabilities in their monitor. Fortuitously, perhaps, the inelastic cross section is essentially constant down to nucleon energies somewhat less than 100 MeV and for lead is 1650 mbn (Chen *et al.* 1955, Preston *et al.* 1960) which is some 21% less than the geometrical cross section, resulting in there being an underestimate of the neutron spectrum by the order of this amount.

While the Hughes and Marsden spectrum is very approximate and subject to many uncertainties it is the only information available and is sufficient as a starting point from which the present calculations can proceed. Unfortunately, however, it cannot be directly applied to the present work, being like most other measurements on low-energy neutrons, a global spectrum, that is, an integrated flux over all angles

made with an essentially flat detector. The present work, by virtue of the configuration of the telescope, is concerned with the neutron intensity in the near-vertical direction, the range of incident zenith angles accepted being relatively small. Taking the neutron intensity to have a zenith angular dependence of the form $I_\theta = I_0 \cos^n\theta$, where I_0 is the vertical intensity, it is easily shown that the relationship between I_0 and the total integrated flux measured by a flat detector I_T is

$$I_V = \frac{n+1}{2\pi} I_T.$$

While it is expected that the value of the angular exponent n will decrease with decreasing neutron energy in the region of evaporation energies (< 50 MeV) it is considered that, for neutron energies experienced in the present work, it will be sensibly constant and in accord with the value of 8 commonly adopted for the higher-energy nucleon component of the cosmic radiation (in fact a value of 8 has already been adopted earlier to enable the aperture of the telescope to be evaluated).

Thus, as a starting point for the ensuing calculations, the vertical intensity spectrum of neutrons has been derived from the Hughes and Marsden global spectrum by scaling it according to the above formula using an exponent of 8. While this is almost certainly justified for energies currently experienced and for higher energies, it will tend to overestimate the vertical intensity at very small energies owing to the then decreasing values of the exponent.

3.3. *The production spectra of single protons and pions*

The production spectrum of single protons $N(E_p)$ from the reaction $n+p \rightarrow p+n$ in a target ${}_zX^A$ of thickness x g cm^{-2} can be written

$$N(E_p)\,dE_p = N(E_n)\,dE_n \frac{N_0}{A} \sigma(E_n)\, x$$

where $\sigma(E_n)$ is the cross section for charge exchange on a nucleus ${}_zX^A$ due to the elementary process $n+p \rightarrow p+n$, and $N(E_n)$ the incident neutron spectrum. $\sigma(E_n)$ was obtained by equating the ratio of the n–p charge exchange cross section and the total n–p cross section to the ratio of $\sigma(E_n)$ and Z/A times the total cross section of neutrons on a nucleus ${}_zX^A$. The total cross section of neutrons on a nucleus was obtained from the elementary cross sections using the calculations of Alexander and Yekutieli (1961). In the charge exchange process it is assumed that the proton takes all the energy of the incident neutron.

In a similar way the production spectrum of single pions $N(E_\pi)$ from the reaction $n+p \rightarrow n+n+\pi^+$ can be written

$$N(E_\pi)\,dE_\pi = \int_{E_{n\,min}}^{E_{n\,max}} N(E_n)\,dE_n \frac{N_0}{A} \sigma(E_n)\, F(E_n, E_\pi)\,dE_\pi$$

where $\sigma(E_n)$ is the cross section for single π^+ production on a nucleus ${}_zX^A$, and $f(E_n, E_\pi)\,dE_\pi$ is the probability of a neutron of energy E_n producing a pion of energy E_π. $F(E_n, E_\pi)$ was evaluated assuming the available kinetic energy in the centre-of-mass system is equally divided between the π^+ and the two neutrons. $\sigma(E_n)$ was determined from the elementary cross sections in the same way as for proton production by charge exchange.

The respective yields of each channel can be seen in figure 3 where the production spectra are given for an assumed target of 1 g cm^{-2} of hydrogen. Taking account of

the relative minimum energies of protons and pions needed to traverse the telescope, as given in table 1(i), the integral yield of protons above threshold in each series is approximately an order of magnitude greater than the corresponding pion yield. Because of the dominance of the charge exchange process over single pion production, and the production spectrum of protons falling very steeply with energy ($\sim E^{-4\cdot8}$), the vast majority of observed events will come from a fairly narrow band of neutron energies—hence allowing reliable estimates to be made of the neutron intensity in localized energy regions.

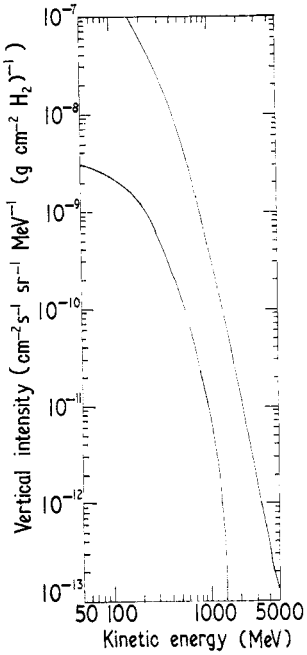

Figure 3. The differential production spectra of protons from the charge exchange reaction, $n+p \rightarrow p+n$ and positive pions from the reaction $n+p \rightarrow n+n+\pi^+$ from neutron interactions in a target of 1 g cm^{-2} of hydrogen. The production spectra were calculated using the Hughes and Marsden (1966) global neutron spectrum which was suitably adopted to give vertical intensities.

Taking into account the complex nature of the target as given in table 1, the number of protons and pions produced in the target during the running time of each series of measurements has been calculated. The attenuation of the incident neutron flux in penetrating the telescope to the target region has been accounted for by straightforward exponential reduction. The number of nucleon inelastic interaction lengths from the top of the telescope to the target region was derived from the work of Chen *et al.* (1955). Interaction rather than attenuation lengths have been used in that any neutron inelastic interaction above the target would result in rejection of the event, either by electronic or visual selection, owing to the production of charged particles. The correction factor to be applied for this loss is 0·48 and the expected numbers of single pions and protons produced in the target after correction are summarized in table 5.

These numbers refer to the production at the target, and before comparison can be made with the observed events a further correction has to be applied for loss due

Table 5. Expected numbers of single protons and pions produced in the target during the running time of each experiment

	N series		M series	
	Energy range	Number	Energy range	Number
Protons	$701 < E_p < 867$ MeV	210·0	$344 < E_p < 551$ MeV	67·6
Protons	$E_p > 867$ MeV	208·5	$E_p > 551$ MeV	39·1
Pions	$E_\pi > 449$ MeV	40·4	$E_\pi > 185$ MeV	8·6

The expected numbers were calculated using the Hughes and Marsden neutron spectrum.

to attenuation of the pions and protons from interactions in traversing the telescope. Unfortunately, this loss cannot be calculated from a simple attenuation law since energy loss by ionization is important in the present case where the majority of the particles are close to the threshold required to penetrate the detector. This correction factor for interaction loss is the most uncertain parameter in the present calculations and to try and optimize the solution two methods of correction have been used and these are discussed in the following section.

3.4. *Interaction losses of protons and pions*

The attenuation of the pion component will be considered first and, as the pion yield is small compared with the proton yield, only a single method of correction has been applied here. It was assumed that all inelastic pion interactions resulted in the loss of that event since, in the present energy region, the absorption and charge exchange reactions are the dominant parts of the inelastic cross section. The probability of a pion inelastic interaction traversing the telescope was evaluated from π^+ nucleus cross sections calculated by Sternheimer (1956), allowances being made for the multi-medium telescope and the energy variation of the penetrating pion. The resulting correction factors were 0·08 and 0·33 for the N and M series respectively. Some pion inelastic interactions would not of course result in the loss of the event but the frequency of such occurrences is estimated to be negligible compared with the total yield of proton events.

Two approaches have been adopted to allow for proton interactions in the telescope, the most important parameter in both being the number of proton interaction lengths in the respective telescopes. Elastic interactions can be disregarded in that they result in small energy transfers having negligible attenuating effect, and thus only inelastic collisions are important. As discussed earlier, the nucleon–nucleus inelastic cross section is essentially energy independent, this simplifying the correction in allowing a constant interaction length to be used over all proton energies. The number of inelastic interaction lengths has been evaluated from inelastic nucleon–nucleus cross sections given by Chen *et al.* (1955), and it is 1·98 and 0·72 for the N and M series respectively.

The first approach relies on being able to separate the observed events into those which have and have not suffered an inelastic interaction. If this is possible a simple method of interaction correction can be applied, to enable comparison between the predicted and observed numbers of noninteracting events, by straightforward exponential reduction of the predicted numbers according to the number of interaction lengths in the telescope. A separation of this sort has in fact been carried out in table 3, where the criterion defining an interaction was that more than one charged particle should emerge from the interaction point, and in table 4 a further subdivision

of the noninteracting events into subrelativistic protons and relativistic pions and protons has been made.

The second approach was to consider all the events expected to trigger the telescope, that is, not only the noninteracting particles but also those which interacted yet still retained sufficient energy to penetrate the remainder of the instrument, thus allowing an immediate comparison with the total observed numbers of events. In the high-energy limit interaction losses can be allowed for by simple attenuation laws, demanding only a knowledge of the particle's interaction length and inelasticity. In the energy range presently studied, energy loss by ionization is important and a Monte Carlo technique has been used.

For convenience the telescope was considered to be uniform throughout for ionization and interaction purposes. The calculation followed the following pattern. A proton was assumed to be produced at the centre of the target and its energy was chosen at random such that it was above the threshold for that particular series of measurements and such that the spectrum of all energies chosen during the calculations was identical with the proton production spectrum given in figure 3. The proton was then followed through a series of collisions, the path length between each being chosen at random according to a procedure which gave probabilities appropriate to the proton interaction length. If the interaction point fell outside the telescope the event was accepted and the calculation restarted with a new proton; otherwise energy loss through ionization in reaching the point of interaction was subtracted and the energy then degraded by KE_p, where K is the proton inelasticity. If the remaining proton energy was insufficient to enable it to penetrate the rest of the telescope the event was classified as lost and a new proton chosen; otherwise the proton was followed through further interactions until either it emerged from the telescope and was accepted or it was absorbed and lost.

The only uncertainty in the calculation of any importance is the proton inelasticity, or inelasticity distribution, for proton–nucleus collisions in the present energy range. No information is available on this quantity and for this reason the calculation was performed for a range of values of K from 0·3 to 0·7 for each telescope configuration. Each individual Monte Carlo calculation for a given value of K contained 1000 trials. This was considered sufficient in that the resulting error was small compared with that introduced from the inherent uncertainty in the inelasticity.

The predicted rates of events given in table 5 have been corrected for interaction losses in the ways previously outlined, and in tables 6 and 7 a final comparison is

Table 6. Comparison of the observed and expected number of non-interacting single-prong events

Series	Particle	Energy (MeV) range	Observed number	Expected number	
N	P	$701 < E_p < 867$	25	28·3	
	P	$E_p > 867$	39	28·8	32·0
	π^-	$E_\pi > 449$		3·2	
M	P	$344 < E_p < 551$	28	32·9	
	P	$E_p > 551$	24	19·1	22·0
	π^+	$E_\pi > 185$		2·9	

The expected numbers were calculated using the Hughes and Marsden neutron spectrum.

made between the observed and expected numbers. Table 6 refers to those events categorized as 'noninteracting' where the predicted numbers have been reduced by straightforward exponential decrease to allow for interactions; table 7 refers to all the observed events, the interaction correction being evaluated by a Monte Carlo method. In the latter case, predicted results are given for assumed values of K of 0·4, 0·5, and 0·6.

Table 7. Comparison of the observed and expected number of all single-prong events

Series	Particle	Energy range (MeV)	Observed number	Expected numbers			
				π^+	P K		
					0·4	0·5	0·6
N	P	$E_p > 701$	93		123·5	102·5	81·6
	π^+	$E_\pi > 449$		3·2			
	Total ($p+\pi^+$)		93		126·7	105·7	84·8
M	P	$E_p > 344$	86		74·8	68·6	62·3
	π^+	$E_\pi > 185$		2·9			
	Total ($p+\pi^+$)		86		77·7	71·5	65·2

The expected numbers were calculated using the Hughes and Marsden neutron spectrum.

From a comparison between the observed and expected numbers, estimates can now be made of the neutron intensity in the energy region under study by adapting the Hughes and Marsden spectrum until satisfactory agreement is obtained between the observed and predicted numbers of events. The way in which this has been performed is discussed in the next section.

3.5. *Estimate of the sea level neutron intensity*

Three evaluations of the neutron intensity have been made for each series of measurements, two of them corresponding to the comparisons in table 6 and the other to that in table 7. While the data in tables 6 and 7 are essentially the same, apart from an excess in table 7 due to the inclusion of the interacting events, it would appear justifiable to calculate intensities for both cases—in that each comparison corresponds to a different energy band, and it enables the selfconsistency of the data to be checked within the bounds of the calculation.

In the case of the lower energy proton samples in table 6, intensities can be readily evaluated and assigned to fairly localized energy regions owing to the sample being purely protonic and the majority being produced in a narrow energy band due to the rapidly falling production spectrum. The intensities have been derived by scaling the Hughes and Marsden spectrum at the mean contributing neutron energy (which is essentially the mean proton production energy in that it has been assumed that the proton takes the whole neutron energy in the change exchange) until agreement was reached between the observed and predicted numbers. The situation is not quite as simple in the cases of the higher-energy particles in table 6 and in the comparison between all the particles in table 7. This arises from there being two types of particle

(protons and pions) in the samples with the bulk of production of each coming from different primary neutron energies. However, the pion component is relatively insignificant compared with the protons and again, therefore, the majority of production comes from a small band of neutron energies. The intensities were derived as before by scaling the Hughes and Marsden spectrum at the mean contributing energy, after initially reducing the derived number by the expected pion yields. The pion yield is so small that any error introduced by the subtraction of this component is unimportant. In the case of the data in table 7 the intensities were evaluated assuming the proton inelasticity to be 0·5. While it must be pointed out that, in the experiment, differential intensities are not being measured, the rapid fall off in the proton production spectrum (figure 3) results in production coming in the main from very localized energy regions and because of this a scaling up into differential intensities seems fairly justified.

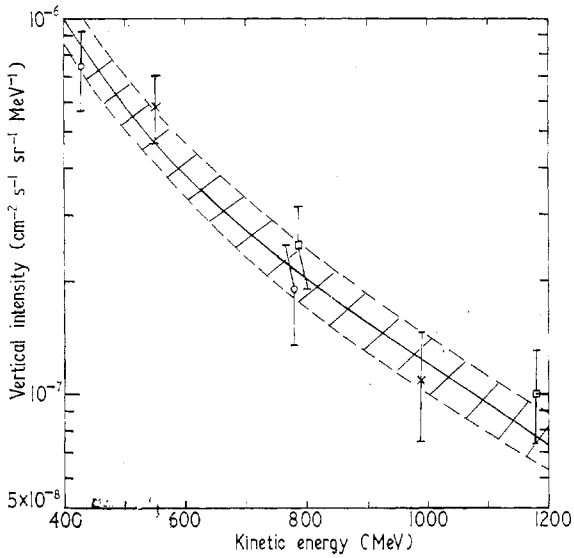

Figure 4. Neutron intensities derived from the present work. The full line is the vertical intensity calculated from the global spectrum of Hughes and Marsden and the hatched area the upper and lower standard deviation bounds to the best fit to the spectrum as suggested by the present work. The circles and squares refer to the data in table 6 containing respectively the lower- and higher-energy proton samples. Interaction losses in both cases were allowed for by simple exponential reduction. The crosses refer to all the data given in table 7 and interaction losses were accounted for by a Monte Carlo technique. All the experimental points are plotted at the mean neutron energy of the energy range contributing to the observed events.

The calculated intensities are shown in figure 4 together with the Hughes and Marsden spectrum converted to vertical intensities in the relevant energy region. The errors quoted on the points allow for both statistical errors on the observed number of events and also errors in the parameters of the calculation used to determine the neutron intensity. The values of the estimated errors in the parameters of the calculations are: a 10% uncertainty in the np charge exchange cross section, a 10% uncertainty in evaluating the number of inelastic interaction lengths both above

and below the target, and, in the case of the Monte Carlo calculation, a 20% uncertainty in the proton–nucleus inelasticity (that is assumed one standard deviation levels of 0·4 and 0·6).

The trend of the points in figure 4 is suggestive of neutron intensities in good agreement with those predicted by Hughes and Marsden. The best fit to the present data was obtained by evaluating the weighted mean increase of the points above the Hughes and Marsden spectrum, this yielding a ratio of $1{\cdot}02 \pm 0{\cdot}07$. In figure 5

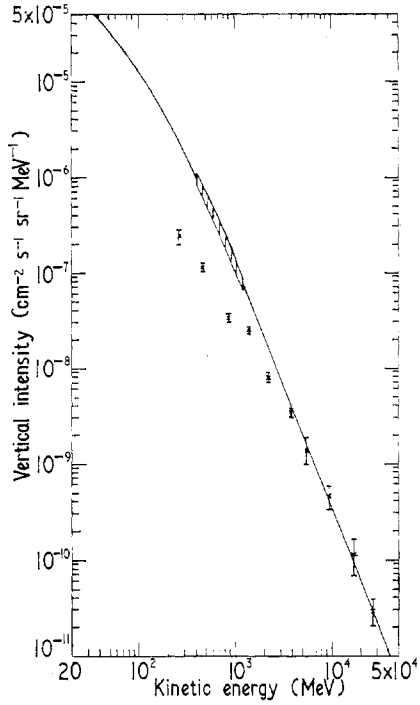

Figure 5. Summary of the sea level vertical neutron and proton spectra in the range 20 MeV to 50 GeV. The full line is the vertical neutron spectrum calculated from the global spectrum given by Hughes and Marsden (1966). The crosses are the proton measurements of Brooke and Wolfendale (1964) and the hatched area the results of the present work for neutrons.

the results of the present work are compared with the Hughes and Marsden estimate of the neutron spectrum, and the measurements of the proton spectrum by Brooke and Wolfendale (1964) are also shown.

4. Conclusions

The charge exchange reaction $n + p \rightarrow p + n$ has been used to measure the energy spectrum of neutrons in the range 0·4–1·2 GeV. Combining the result with the low-energy neutron measurements of Hess *et al.* (1959) and the high-energy proton measurements of Brooke and Wolfendale (1964), the best estimate of the sea level neutron spectrum has been made in the range 20 MeV to 40 GeV. From figure 5 it can be seen that ionization loss can only be neglected in considering the propagation of nucleons of energy greater than 5 GeV through the earth's atmosphere.

Acknowledgments

Professor G. D. Rochester and Professor A. W. Wolfendale are thanked for encouraging this work which was supported by a grant from the Science Research Council.

References

ALEXANDER, G., and YEKUTIELI, G., 1961, *Nuovo. Cim.*, **19,** 103–17.
ASHTON, F., and COATS, R. B., 1968, *J. Phys.* A: *Gen. Phys.*, **1,** 169–71.
ASHTON, F., EDWARDS, H. J., and KELLY, G. N., 1969, *Phys. Lett.*, **29B,** 249–51.
BROOKE, G., and WOLFENDALE, A. W., 1964, *Proc. Phys. Soc.*, **83,** 843–51.
CHEN, F. F., LEWITT, C. P., and SHAPIRO, A. M., 1955, *Phys. Rev.*, **99,** 857–71.
GALBRAITH, W., 1969, *Rep. Prog. Phys.*, **32,** 547–606.
HESS, N. H., PATTERSON, H. W., and WALLACE, R., 1959, *Phys. Rev.*, **116,** 445–57.
HUGHES, E. B., and MARSDEN, P. L., 1966, *J. geophys. Res.*, **71,** 1435–44.
KELLY, G. N., 1969, *PhD Thesis*, Durham University.
LINDENBAUM, S. J., 1957, *Ann. Rev. Nucl. Sci.*, **7,** 317–48.
MANNING, G., *et al.*, 1966, *Nuovo Cim.*, **40,** 167–88.
PRESTON, W. M., WILSON, R., and STREET, J. C., 1960, *Phys. Rev.*, **118,** 579–88.
SINGER, S. F., 1958, *Prog. Cosmic Ray Phys.*, **4,** 205–335.
STERNHEIMER, R. M., 1956, *Phys. Rev.*, **101,** 384–7.